

Ballistic and diffuse transport through a ferromagnetic domain wall

Arne Brataas[†]

*Department of Applied Physics and Delft Institute of Microelectronics and Submicronotechnology,
Delft University of Technology, Lorentzweg 1, 2628 CJ Delft, The Netherlands*

Gen Tatara

Graduate School of Sciences, Osaka University, Toyonaka, Osaka 560, Japan

Gerrit E. W. Bauer

*Department of Applied Physics and Delft Institute of Microelectronics and Submicronotechnology,
Delft University of Technology, Lorentzweg 1, 2628 CJ Delft, The Netherlands
(February 7, 2008)*

We study transport through ballistic and diffuse ferromagnetic domain walls in a two-band Stoner model with a rotating magnetization direction. For a ballistic domain wall, the change in the conductance due to the domain wall scattering is obtained from an adiabatic approximation valid when the length of the domain wall is much longer than the Fermi wavelength. In diffuse systems, the change in the resistivity is calculated using a diagrammatic technique to the lowest order in the domain wall scattering and taking into account spin-dependent scattering lifetimes and screening of the domain wall potential.

75.60.Ch, 73.50.Bk, 75.70.-i

I. INTRODUCTION

In a ferromagnet, domains with different directions of the magnetization are favored by the long-range magnetic dipolar interaction. The boundary between the domains, the domain walls (DW's), are a source of magnetoresistance that recently has attracted experimental¹⁻⁵ and theoretical interest.⁶⁻⁸

For ballistic systems, where the electron mean free path is longer than the system size, first-principles band-structure calculations have shown that the DW resistance is enhanced due to the nearly degenerate bands at the Fermi energy.⁸ The rotating magnetization direction causes an effective potential barrier for the electrons which increase the resistance. Recently large DW resistance in ballistic Ni nanocontacts has been measured⁹ in agreement with the predictions in Ref. 8.

In the diffuse transport regime Cabrera and Falicov¹⁰ interpreted transport through a single DW as a tunneling process and the corresponding MR was found to be exponentially small. Berger¹¹ modelled the domain wall scattering as a force on the magnetic moment of the conduction electrons. Tatara and Fukuyama⁶ calculated the DW conductivity for spin-independent scattering lifetimes. Levy and Zhang⁷ pointed out that spin-dependent

impurity scattering can strongly enhance the DW resistivity.

Beyond the semiclassical transport theories, Tatara and Fukuyama⁶ predict a negative DW resistivity as a result of the reduced weak localization correction due to the decoherence of the electrons by the scattering off the domain wall. However, quantum interference effects do not explain the experiments in Refs. 3,4, where the negative DW resistance persists up to high temperature where the inelastic scattering length is shorter than the mean free path. It has been suggested by Ruediger et al.¹² that the experimentally observed negative DW resistance is an extrinsic effect caused by the interplay between orbital effects due to the internal magnetic fields and surface scattering. Recently, it was also demonstrated that the large negative domain wall resistance of Co films¹ is due to MR resistivity anisotropy.¹³

It is the purpose of the present paper to give a detailed account of the transport through a domain wall both in the ballistic and the diffuse regime in a two-band Stoner model. In the ballistic transport regime, the transport through the magnetic domain wall can be treated by an adiabatic approximation similar to the one used for transport through a quantum point contact. In the diffuse regime we will use the diagrammatic technique introduced in Ref. 6 and generalize it to the case of asymmetric impurity scattering life-times (but without localization effects⁶) and screening of the domain wall potential. Our results, although more general, reduce in the case of strong spin splitting to results that are very similar to those obtained in Ref. 7 using a Boltzmann equation. We explain why the results of the two methods differ. Some results have been published already in a brief report and a conference proceedings.^{8,14} Here we give an in depth discussion of the results including the technical details of the derivations.

The paper is organized in the following way. The two-band Stoner model for the ferromagnet with a rotating magnetic field and how it can be reduced to a more tractable form by a local gauge transformation is discussed in section II. The ballistic transport regime is discussed in section III and the diffuse transport regime in section IV. We give our conclusions in section V. The

appendices include the adiabatic approximation which can be used in the ballistic situation, recipes for the calculation of the frequency summation of the Feynman diagrams, and the spin-spiral case which can be exactly diagonalized.

II. MODEL

Throughout, we will use an effective 2-band model to describe the ferromagnet with the Hamiltonian

$$H = \int d\mathbf{r} \Psi_0^\dagger(\mathbf{r}) \left[-\frac{\hbar^2}{2m} \nabla^2 + \mu_B \mathbf{H}(\mathbf{r}) \cdot \boldsymbol{\sigma} \right] \Psi_0(\mathbf{r}), \quad (1)$$

where μ_B is the Bohr magneton, σ_x, σ_y and σ_z are the Pauli spin matrices, $\mathbf{H}(\mathbf{r})$ is the effective magnetic field arising from the electronic exchange interaction, the magnetic dipole interaction, and the external magnetic field and $\Psi_0(\mathbf{r})$ is the 2-component spinor wave function. The direction of the effective magnetic field is represented by a rotation angle $\theta(z)$ which varies along the z -direction. The spin-orbit interaction and the Lorentz force due to the internal magnetization are disregarded, since experimentally the DW magnetoresistance can be separated from the anomalous magnetoresistance (AMR) and the orbital magnetoresistance (OMR).⁴ We use a local gauge transformation⁶ $\Psi_0(\mathbf{r}) = U(\mathbf{r})\Psi(\mathbf{r})$, where

$$U(\mathbf{r}) = \cos(\theta/2)\sigma_z + \sin(\theta/2)\sigma_x \quad (2)$$

and introduce the Fourier transform of the change of the direction of the magnetic field $a(z) \equiv d\theta(z)/dz = \sum_q \exp(iqz)a_q$. After the gauge transformation (2) the Hamiltonian (1) becomes $\tilde{H} = U^\dagger H U = H_0 + V$. The unperturbed term is

$$H_0 = \sum_{\mathbf{k}s} (\epsilon_{\mathbf{k}}^s - \mu) c_{\mathbf{k}s}^\dagger c_{\mathbf{k}s}, \quad (3)$$

where $s = +$ ($s = -$) denotes spin-up (spin-down) states, $\epsilon_{\mathbf{k}}^s = \hbar^2 k^2/2m - s\Delta$ and the spin-splitting is $\Delta = \mu_B |\mathbf{H}|$. The interaction with the DW is⁶

$$V = \frac{\hbar^2}{2m} \frac{1}{4} \sum_{\mathbf{k}q q' s} a_{q-q'} a_{q'} c_{\mathbf{k}+q\mathbf{z}s}^\dagger c_{\mathbf{k}s} + \frac{\hbar^2}{2m} \sum_{\mathbf{k}q s s'} \left(k_z + \frac{q}{2} \right) a_q c_{\mathbf{k}+q\mathbf{z}s}^\dagger (\sigma_y)_{s,s'} c_{\mathbf{k}s'}, \quad (4)$$

where $\hat{\mathbf{z}}$ is a unit vector in the z -direction and $k_z = \mathbf{k} \cdot \hat{\mathbf{z}}$.

III. BALLISTIC TRANSPORT

Transport through the domain wall is ballistic when the system size is smaller than the mean free path. In

this regime, the transport properties can be described by the Landauer conductance,

$$G = \frac{e^2}{h} \sum_{\mathbf{k}_\parallel ss'} T_{\mathbf{k}_\parallel}^{ss'}, \quad (5)$$

where $T_{\mathbf{k}_\parallel}^{ss'}$ is the transmission probability for an electron in the transverse mode \mathbf{k}_\parallel to pass the domain wall from spin-state s' to spin-state s . Domain walls in transition metals are much thicker than the Fermi wavelength (the length of the domain wall is $\lambda_w = 40\text{nm}$ (Fe), $\lambda_w = 100\text{nm}$ (Ni), $\lambda_w = 15\text{nm}$ (Co) and the Fermi wavelength is roughly $\lambda_F \sim 0.2\text{ nm}$). The transmission probability can therefore be calculated with the aid of an adiabatic approximation on the eigenstates of the Hamiltonian after the gauge transformation (2) (see Appendix A). The domain wall is then equivalent to an effective potential barrier for the electrons. The conductance is determined by the minimum number of propagating modes, which is where the gradient of the rotating magnetic field has its maximum value, $a(z) \equiv d\theta(z)/dz \rightarrow a_{\max}$ (for details see Appendix A). The conductance can then be found from the conductance of a spin-spiral with gradient a_{\max} , which has the dispersion $E_{\max}^\pm = \hbar^2/(2m)[k^2 + a_{\max}^2/4 \pm (k_z^2 a_{\max}^2 + p^4)^{1/2}]$, and the conductance is

$$G = \frac{e^2}{2} \sum_{\mathbf{k}s} |v_s| \delta(E_{\max}^s - E_F), \quad (6)$$

where $v_s = \partial E_s/(\hbar \partial k_z)$ is the group velocity. Carrying out the integration, we find the domain wall resistance $R_w/R_0 = R - R_0$ ($1/R = G$, $1/R_0 = G_0 = (e^2 A \bar{k}_F^2)/(2\pi\hbar)$):

$$\frac{R_w}{R_0} = \begin{cases} a_{\max}^2/(4\bar{k}_F^2) & a_{\max}^2 \leq 2p^2 \\ p^2/\bar{k}_F^2 - p^4/(a_{\max}^2 \bar{k}_F^2) & a_{\max}^2 > 2p^2 \end{cases}, \quad (7)$$

where $\hbar^2 \bar{k}_F^2/(2m) \equiv E_F$ and $\Delta \equiv \hbar^2 p^2/(2m)$. The screening of the domain wall potential discussed below is not important for the calculation of the conductance, since by a calculation following the lines in section IV, we find that the shift in the chemical potential due to the rotating magnetization is $\delta\mu \approx -(1/48)E_w(\Delta/E_F)^2 + \mathcal{O}(\Delta/E_F)^3$. The conductance is $G \sim k_F^2 \sim \mu$, and therefore screening gives a vanishing small contribution to the change in the resistance when the splitting is sufficiently small, $\delta R_\mu/R_0 \approx (1/48)(E_w/E_F)(\Delta/E_F)^2$.

Using parameters for Fe, Ni and Co ($\lambda_w = 40\text{ nm}$, $\lambda_w = 100\text{ nm}$, $\lambda_w = 15\text{ nm}$, respectively), we find $R_w/R = 0.0008\%$, $R_w/R_0 = 0.0001\%$, $R_w/R_0 = 0.008\%$ respectively. Within the 2-band model, the ballistic domain wall scattering is thus very weak. In first-principles band structure calculations these small numbers are enhanced by orders of magnitude due to the (near) degeneracy of the energy bands at the Fermi level.⁸

IV. DIFFUSE TRANSPORT

When the system size is much larger than the mean free path, the transport is in the diffuse regime. We assume that the electrons are subject to spin-dependent scattering, which is modelled by short-range scatters giving rise to spin-dependent life-times τ_+ and τ_- for spin-up and spin-down states, respectively, which will be treated as adjustable parameters.

We study the current in the z -direction. The current operator transformed by the local spin rotation $U(\mathbf{r})$ in (2) is $\tilde{J} = U^\dagger J U = J_0 + J_g$. The unperturbed current operator is

$$J_0 = \frac{e\hbar}{m} \sum_{\mathbf{k}s} k_z c_{\mathbf{k}s}^\dagger c_{\mathbf{k}s} \quad (8)$$

and due to the local gauge transformation⁶

$$J_g = \frac{e\hbar}{2m} \sum_{\mathbf{k}qss'} a_q c_{\mathbf{k}+q\mathbf{z}s}(\sigma_y)_{s,s'} c_{\mathbf{k}s'} . \quad (9)$$

The conductivity is calculated from the Kubo formula.

$$\sigma(\omega) = \frac{i}{\omega} \left[\Pi(\omega) + \frac{n_0 e^2}{m} \right], \quad (10)$$

where $n_0 = N/V$ is the electron density, N is the number of electrons and V is the volume of the system. The current-current correlation function $\Pi(\omega)$ is obtained by an analytical continuation ($i\omega_l \rightarrow \omega + i\delta$, $\delta \rightarrow 0^+$) from the Matsubara correlation function

$$\Pi^l = -\frac{1}{V} \frac{1}{\hbar} \int_0^{\beta\hbar} e^{i\omega_l t} \langle T_\tau \tilde{J}(\tau) \tilde{J}(0) \rangle, \quad (11)$$

where $1/\beta = k_B T$, k_B is the Boltzmann constant, T is the temperature and T_τ is the τ -ordering operator. We will only study the DC conductivity at low temperatures by letting $\omega \rightarrow 0$ and $T \rightarrow 0$. The relevant Feynman diagrams to the lowest order in the scattering by the domain wall were identified in Ref. 6 and are shown in Fig. 1. Diagram (0) represents the zeroth order Drude contribution, diagram (1) is due to the correlation of the correction to the conductivity operator (9), diagrams (2) and (4) are self-energy corrections from the interaction Hamiltonian (4) to the electron Green's function, diagram (5) is a vertex correction, and diagram (3) is the correlation of the change in the current operator (9) and the interaction Hamiltonian (4). The electron Green's function appearing in the Feynman diagrams in Fig. 1 is a configurational average over impurity positions, *e.g.* the retarded Green's function is

$$G_{\mathbf{k}s}^R(\omega) = \frac{1}{\hbar\omega - \epsilon_{\mathbf{k}}^s + i\hbar/2\tau_s}. \quad (12)$$

The scattering lifetimes of the states at the Fermi energy due to the impurity scattering τ_s are assumed to be isotropic but may be spin-dependent.¹⁵

The DC conductivity of a single-domain ferromagnet is

$$\sigma_0 = \frac{e^2}{V} \sum_{\mathbf{k}s} \left(\frac{\partial \epsilon_{\mathbf{k}s}}{\partial k_z} \right)^2 \delta(\epsilon_{\mathbf{k}s} - \mu_0) \tau_s \quad (13)$$

$$= \frac{e^2}{m} (n_+ \tau_+ + n_- \tau_-), \quad (14)$$

where μ_0 is the bulk chemical potential, n_+ (n_-) is the electron density of spin-up (spin-down) states and τ_+ (τ_-) is the scattering life-time of spin-up (spin-down) states.

There are two contributions to the conductivity which to the lowest order in the domain wall scattering are additive. Firstly, screening shifts the chemical potential and induces a DW conductivity in (13). Secondly, the electrons are directly scattered by the domain wall by the interaction term (4) and the gauge transformed current operator (9).

Since the width of domain walls in transition metals is much larger than the screening length, electroneutrality dictates that the electron density to a good approximation is the same in the presence or absence of the DW, but the chemical potential differs. This is in contrast to the treatment in Refs. 6,7, where the chemical potential is assumed to be the same in the presence or absence of the DW. The change in the conductivity due to the chemical potential shift can be found from (13) setting $\mu_0 \rightarrow \mu_0 + \delta\mu$:

$$\delta\sigma_0 = \delta\mu \frac{e^2}{m} \sum_s N_s \tau_s, \quad (15)$$

which to lowest order in the domain wall scattering may be added to the DW conductivity. Here $N_s = mk_F^s/(2\pi^2\hbar^2)$ is the electron density of states at the Fermi energy, k_F^s is the spin-dependent Fermi wave vector related to the spin-dependent electron density by $n_s = (k_F^s)^3/(6\pi^2)$ and we also introduce $\epsilon_F^s \equiv \hbar^2(k_F^s)^2/(2m)$.

We proceed by calculating the chemical potential shift due to the rotating magnetization. The zeroth order contribution to the electron density is $n_0 = \sum_{\mathbf{k}s} \theta(\mu - \epsilon_{\mathbf{k}}^s)/V$, where $\theta(x)$ is the Heaviside step-function. The Feynman diagrams of the contributions to the electron density in the lowest order interaction with the domain wall are shown in Fig. 2. Diagram (A) is due to the first term in (4) and diagram (B) is due to the second order contribution of the second term in (4). Combining the two terms, the second order contribution to the electron density is

$$n_2 = \frac{\hbar^2}{2mV} \sum_{\mathbf{k}q} |a_q|^2 \left(\frac{\hbar^2 k_z^2/2m}{2\Delta(\mathbf{k}q)} - \frac{1}{4} \right) \delta(\epsilon_{\mathbf{k}-}^s - \mu), \quad (16)$$

where $2\Delta(\mathbf{k}q) = \epsilon_{\mathbf{k}+}^s - \epsilon_{\mathbf{k}-}^s$ and $\mathbf{k}_\pm = \mathbf{k} \pm (q/2)\hat{\mathbf{z}}$. Since the DW is much thicker than the Fermi wavelength, we disregard the wave-vector dependence (q) on the electron states at the Fermi level and introduce the energy parameter for the domain wall, $E_w = \sum_q \hbar^2 |a_q|^2/(2m)$, *e.g.*

with $\cos \theta = \tanh(z/\lambda_W)$, $E_w = \pi \hbar^2 / (L \lambda_W m)$, where $n_W = 1/L$ is the “density” of the domain wall. The chemical potential shift follows from $n_0 + n_2 = n$, where n is the electron density,

$$\delta\mu = E_w \left[\frac{1}{4} - \frac{\sum_s s N_s \epsilon_F^s}{6\Delta \sum_s N_s} \right]. \quad (17)$$

The correction in the conductivity (15) due to the chemical potential shift becomes

$$\delta\sigma_0 = \frac{e^2 E_w}{m} \sum_s N_s \tau_s \left[\frac{1}{4} - \frac{\sum_s s N_s \epsilon_F^s}{6\Delta \sum_s N_s} \right]. \quad (18)$$

The corrections to the current-current correlation function from diagrams (1–5) are

$$\Pi_1^l = \frac{e^2 \hbar^2}{4m^2 V} \sum_{\mathbf{k}q\mathbf{s}} |a_q|^2 \pi_1^l(\mathbf{k}q\mathbf{s}) \quad (19a)$$

$$\Pi_2^l = \frac{e^2 \hbar^4}{8m^3 V} \sum_{\mathbf{k}q\mathbf{s}} |a_q|^2 k_z^2 \pi_2^l(\mathbf{k}q\mathbf{s}) \quad (19b)$$

$$\Pi_3^l = \frac{e^2 \hbar^4}{2m^3 V} \sum_{\mathbf{k}q\mathbf{s}} |a_q|^2 (k_z - \frac{q}{2}) k_z \pi_3^l(\mathbf{k}q\mathbf{s}) \quad (19c)$$

$$\Pi_4^l = \frac{e^2 \hbar^6}{4m^4 V} \sum_{\mathbf{k}q\mathbf{s}} |a_q|^2 (k_z - \frac{q}{2})^2 k_z^2 \pi_4^l(\mathbf{k}q\mathbf{s}) \quad (19d)$$

$$\Pi_5^l = \frac{e^2 \hbar^6}{4m^4 V} \sum_{\mathbf{k}q\mathbf{s}} |a_q|^2 k_z^2 (k_z^2 - \frac{q^2}{4}) \pi_5^l(\mathbf{k}q\mathbf{s}), \quad (19e)$$

where the frequency summations are defined by

$$\pi_1^l = \frac{1}{\beta} \sum_n G_{\mathbf{k}-s}^{n+l} G_{\mathbf{k}+s}^n \quad (20a)$$

$$\pi_2^l = \frac{1}{\beta} \sum_n [G_{\mathbf{k}s}^{n+l} G_{\mathbf{k}s}^{n+l} G_{\mathbf{k}s}^n + (l \rightarrow -l)] \quad (20b)$$

$$\pi_3^l = \frac{1}{\beta} \sum_n [G_{\mathbf{k}-s}^{n+l} G_{\mathbf{k}+s}^{n+l} G_{\mathbf{k}-s}^n + (l \rightarrow -l)] \quad (20c)$$

$$\pi_4^l = \frac{1}{\beta} \sum_n [G_{\mathbf{k}-s}^{n+l} G_{\mathbf{k}+s}^{n+l} G_{\mathbf{k}-s}^{n+l} G_{\mathbf{k}-s}^n + (l \rightarrow -l)] \quad (20d)$$

$$\pi_5^l = \frac{1}{\beta} \sum_n G_{\mathbf{k}-s}^{n+l} G_{\mathbf{k}+s}^{n+l} G_{\mathbf{k}-s}^n G_{\mathbf{k}+s}^n. \quad (20e)$$

In the low impurity density limit the energy splitting between the bands is larger than the broadening of the bands due to the impurity scattering, $\Delta\tau/\hbar \gg 1$. The frequency sums (20) are evaluated in Appendix B, where the weak wave-vector dependence on the electron states at the Fermi level is disregarded consistent with the treatment of the chemical potential shift above. Carrying out the Matsubara frequency sums over the internal energies at low temperature, we find that the correction to the DC conductivity due to the DW is

$$\sigma_1 = 0 \quad (21a)$$

$$\sigma_2 = -\frac{e^2 E_w}{m} \sum_s N_s \tau_s \frac{1}{4} \quad (21b)$$

$$\sigma_3 = -\frac{e^2 E_w}{m} \sum_s N_s \tau_s \frac{2}{3} s \frac{\epsilon_F^s}{\Delta} \quad (21c)$$

$$\sigma_4 = \frac{e^2 E_w}{m} \sum_s N_s \tau_s \left[\frac{s \epsilon_F^s}{2\Delta} - \left(\frac{\epsilon_F^s}{\Delta} \right)^2 \frac{\tau_+ + \tau_-}{10\tau_{-s}} \right] \quad (21d)$$

$$\sigma_5 = \frac{e^2 E_w}{m} \sum_s N_s \tau_s \frac{1}{5} \left(\frac{\epsilon_F^s}{\Delta} \right)^2. \quad (21e)$$

The contribution to the conductivity from the diagrams (1-5) in Fig. 1 is

$$\sum_{i=1}^5 \sigma_i = -\frac{e^2 E_w}{m} \sum_s N_s \tau_s \times \left[\frac{1}{4} + \frac{1}{6} s \frac{\epsilon_F^s}{\Delta} - \frac{1}{10} \left(\frac{\epsilon_F^s}{\Delta} \right)^2 \left(1 - \frac{\tau_s}{\tau_{-s}} \right) \right]. \quad (22)$$

The DW resistivity can be found from $\rho_w = -\sigma_w \rho_0^2$, where the DW conductivity change due to the rotating magnetic field is $\sigma_w = \delta\sigma_0 + \sum_{i=1}^5 \sigma_i$:

$$\rho_w = \frac{e^2 \rho_0^2 E_w}{6m} \sum_s N_s \tau_s \times \left[\frac{\delta\epsilon_F}{\Delta} + \frac{s \epsilon_F^s}{\Delta} - \frac{3}{5} \left(\frac{\epsilon_F^s}{\Delta} \right)^2 \left(1 - \frac{\tau_s}{\tau_{-s}} \right) \right], \quad (23)$$

where $\delta\epsilon_F = \sum_s s N_s \epsilon_F^s / \sum_s N_s$. The first term in (23) is always positive, but the second and the third terms can be negative when the relaxation time of the minority spin electrons is longer than the relaxation time for the majority spin electrons. However, as will be demonstrated below, the domain wall resistivity given by (23) is always positive. Our speculation about the possibility of a negative domain wall resistance in Ref. 14 is thus not justified from Eq. (23) only. The result (23) differs from that obtained in Ref. 6 for spin-independent relaxation times $\tau_s = \tau$, where screening was not taken into account, *i.e.* a constant chemical potential and not a constant electron density was assumed. The result also differs from the calculation in Ref. 7 based on the Boltzmann equation. We believe that this latter discrepancy is because in Ref. 7 screening as well as the effect of the gauge transformation on the current operator (9) are neglected. The latter corresponds to the neglect of the diagrams (1) and (3) in Fig. 1. For sufficiently weak impurity scattering and/or a large spin splitting ($\Delta\tau/\hbar \gg 1$) the contribution from diagram (1), Eq. (21a), vanishes, so only in this limit the omission of this diagram is justified. Furthermore, the difference in the Fermi wave vectors for the spin-up and spin-down electrons was disregarded in parts of the calculations in Ref. 7 and an approximation

was introduced in order to solve the integral equation for the Boltzmann equation. Indeed, assuming small spin splittings ($\Delta/\epsilon_F \ll 1$, but $\Delta\tau/\hbar \gg 1$) in Eq. (23), we obtain

$$\frac{\rho_w}{\rho_0} \approx \frac{3E_w E_F}{20\Delta^2} \frac{(\tau_+ - \tau_-)^2}{\tau_+ \tau_-} \quad (24)$$

which is very similar, but not identical to the result in Ref. 7. In this limit, the domain wall resistivity increases quadratically with the asymmetry in the spin-up and spin-down scattering lifetimes as pointed out in Ref. 7. For larger spin splitting, Eq. (23) should be used.

It is also interesting to study the domain wall resistivity when the spin-splitting is large, $2\Delta > \mu$, which is the case for a half-metallic ferromagnet in which the minority spin density of states vanishes $N_- = 0$. In this regime we find

$$\frac{\rho_w}{\rho_0} = \frac{E_w}{\mu} \left[\frac{\mu}{2\Delta} - \frac{3}{5} \left(\frac{\mu}{2\Delta} \right)^2 \left(1 - \frac{\tau_+}{\tau_-} \right) \right]. \quad (25)$$

The first term in (25) can be interpreted as additional intraband scattering in the majority spin channel due to the rotating magnetization and the second term as virtual transport in the minority spin channel which has a negative contribution when $\tau_- > \tau_+$. The domain wall resistivity (25) is always positive. In the limit of large spin-splittings $\Delta \gg \mu$ the domain wall resistivity vanishes, since the coupling between the bands becomes vanishing small. Note that the present formalism is valid only for wide walls, since the domain wall scattering is treated as a perturbation.

Our perturbative result (23) can be checked against an exact calculation for a spin-spiral, $d\theta(z)/dz = a_0$, $a_q = a_0 \delta_{q,0}$ with spin-independent life-times $\tau_s \rightarrow \tau$. The detailed calculation is shown in Appendix C. The Hamiltonian is diagonalized in spin space by $\mathbf{u}_\pm = \mathcal{N}_\pm [1, i(1 \mp \sqrt{1 + \alpha^2})/\alpha]^T$, where \mathcal{N}_\pm is a normalization constant, $\alpha = k_z a_0 / p^2$ and $\Delta = \hbar^2 p^2 / 2m$. The corresponding eigenvalues are $E_{\mathbf{k}}^\pm = (\hbar^2 / 2m) (k^2 + a_0^2 \mp \sqrt{k_z^2 a_0^2 + p^4})$. The (Drude) resistivity can be calculated from the Kubo formula,

$$\rho_w = \frac{e^2 \rho_0^2 E_w}{2m\Delta} \tau (n_+ - n_-). \quad (26)$$

This is in exact agreement with Eq. (23) for $a_q = a_0 \delta_{q,0}$ when $\tau_+ = \tau_-$; a good indication of the correctness of our perturbation approach. The calculations in Refs. 6,7 disagree with the exact result (26) presumably due to the reasons outlined above.

The result for the domain wall resistivity (23) can be analyzed by introducing $k_F^+ = \sqrt{\gamma} k_F$, $k_F^- = k_F / \sqrt{\gamma}$, $\tau_+ = \sqrt{\eta} \tau$, $\tau_- = \tau / \sqrt{\eta}$, where $\gamma = k_F^+ / k_F^-$ is a measure of the polarization of the ferromagnet, $\eta = \tau_+ / \tau_-$ is a measure of the asymmetry of the scattering life-times, k_F is the average Fermi wave vector and τ is the

average scattering life-time. The domain wall resistivity is proportional to $\kappa = E_w / 4E_F$. Typically in Fe $k_F \sim 1.7 \text{\AA}^{-1}$, $\lambda_W \sim 300 \text{\AA}$ and $n_w \sim 2.5 \mu m^{-1}$ giving $\kappa \sim 10^{-6}$, which means that the domain wall scattering for symmetric scattering life-times is very weak. However, as pointed out in Ref. 7, the domain wall resistivity can become appreciable larger when taking into account the life-time asymmetry of the carriers. We show in Fig. 3 the scaled domain wall resistivity $\rho_w / (\kappa \rho_0)$ as a function of the asymmetric scattering life-times τ_+ / τ_- in the case of a small spin polarization $\gamma = 1.01$ (solid line), intermediate spin polarization $\gamma = 1.20$ (dashed line) and large spin polarization $\gamma = 10.0$ (dotted line). For a larger spin-polarization, the domain wall resistivity naturally becomes asymmetric in the relative difference in the scattering lifetimes τ_+ and τ_- . The domain wall resistivity becomes noticeable for asymmetric life-times and can become of the order $\rho_w / \rho_0 \sim 1\%$.

V. CONCLUSIONS

We studied the contribution of domain wall scattering on the transport properties of a ferromagnet using an effective 2-band model.

In a diffuse ferromagnet, the domain wall resistivity is calculated from the Kubo formula. The domain wall resistivity is found to be strongly enhanced when the scattering lifetimes of the majority spins and minority spins are different, in agreement with the results in Ref. 7.

In the ballistic regime, we have demonstrated how the domain wall scattering creates an effective barrier that the electrons must pass. The results from the 2-band model give only very small corrections to the resistance of the system.

First-principle band-structure calculations have shown that the domain wall resistance can be increased by orders of magnitude in the ballistic regime.⁸ It would be interesting to perform a realistic band-structure calculation also for diffuse systems. However, the generalization of our 2-band results turns out to be cumbersome.¹⁴

ACKNOWLEDGMENTS

This work is part of the research program for the ‘‘Stichting voor Fundamenteel Onderzoek der Materie’’ (FOM), which is financially supported by the ‘‘Nederlandse Organisatie voor Wetenschappelijk Onderzoek’’ (NWO). We acknowledge benefits from the TMR Research Network on ‘‘Interface Magnetism’’ under contract No. FMRX-CT96-0089 (DG12-MIHT) and support from the NEDO joint research program (NTDP-98). We acknowledge stimulating discussion with Jaap Caro, Ramon P. van Gorkom, Junichiro Inoue, Paul J. Kelly, and Andrew D. Kent.

APPENDIX A: ADIABATIC APPROXIMATION

In the ballistic regime, it is most convenient to start with the Hamiltonian in its first quantized form, which after the gauge transformation (2) reads $\hat{H} = H_0 + V$:⁷

$$H_0 = -\frac{\hbar^2}{2m}\nabla^2 + \Delta\sigma_z, \quad (\text{A1})$$

$$V = \frac{\hbar}{2m}\sigma_y a(z)p_z - \frac{i\hbar^2}{2m}\sigma_y a'(z) + \frac{\hbar^2}{8m}a^2(z), \quad (\text{A2})$$

where $a(z) = d\theta(z)/dz$ is the gradient of the rotating angle of the magnetization and $a'(z) = d^2\theta(z)/dz^2$. The wave function can be written as

$$\Psi(\mathbf{r}) = \phi(\boldsymbol{\rho}) \left[A_{\mathbf{k}}(z) \begin{pmatrix} 1 \\ 0 \end{pmatrix} + B_{\mathbf{k}}(z) \begin{pmatrix} 0 \\ 1 \end{pmatrix} \right], \quad (\text{A3})$$

where $\phi(\boldsymbol{\rho}) = A^{-1/2} \exp(i\mathbf{k}_{\parallel}\boldsymbol{\rho})$ is the transverse part of the wave function ($\mathbf{k} = (\mathbf{k}_{\parallel}, k_z)$), $A_{\mathbf{k}}(z)$ is the spin-up like longitudinal amplitude and $B_{\mathbf{k}}(z)$ is the spin-down like longitudinal amplitude. The Schrödinger equation then becomes

$$\begin{pmatrix} -\frac{d^2}{dz^2} - \omega_+^0 & -a\frac{d}{dz} - \frac{a'}{2} \\ a + \frac{a'}{2} & -\frac{d^2}{dz^2} - \omega_-^0 \end{pmatrix} \cdot \begin{pmatrix} A_{\mathbf{k}} \\ B_{\mathbf{k}} \end{pmatrix} = \begin{pmatrix} 0 \\ 0 \end{pmatrix}, \quad (\text{A4})$$

where

$$\omega_{\pm}^0 = k_{\perp}^2 - a(z)^2/4 \mp p^2, \quad (\text{A5})$$

$k_{\perp}^2 = 2mE_F/\hbar^2 - k_{\parallel}^2$, and E_F is the Fermi energy. The off-diagonal terms in (A4) describe the coupling between the spin-up and spin-down like states. In the case of a spin-spiral, $a'(z) = 0$, the eigenstates can be found to be $A_{\mathbf{k}} = A_{\mathbf{k}}^0 \exp(ik_z z)$, $B_{\mathbf{k}} = B_{\mathbf{k}}^0 \exp(ik_z z)$, where the dispersion of the modes, k_z , are determined by

$$k_{\perp}^2 = k_z^2 + a^2/4 \pm \sqrt{p^4 + q^2 k_z^2}, \quad (\text{A6})$$

The coupling is weak when the gradient of the spin rotation gradient is slow compared to the Fermi wave length. This permits us to make use of a multiple scale analysis (or adiabatic approximation).¹⁶ This analysis is done by introducing the small parameter ϵ , so that $\omega(z) \rightarrow \omega(\epsilon z)$, $a(z) \rightarrow a(\epsilon z)$ and $da/dz \rightarrow \epsilon da/dz$ and we introduce the new variable $Z = g(\epsilon z)/\epsilon$, where $g(\epsilon z)$ is a scaling function.¹⁶ We expand the longitudinal function $A_{\mathbf{k}}(z)$ and $B_{\mathbf{k}}(z)$ to the lowest order in the small parameter ϵ , $A_{\mathbf{k}}(z, Z) = a_{\mathbf{k}}^0(Z, z) + \mathcal{O}(\epsilon)$. To the lowest order in the small parameter ϵ , the equation to solve is thus

$$\begin{pmatrix} \frac{d^2}{dZ^2} + \frac{\omega_+^0}{(g')^2} & \frac{a}{g'} \\ -\frac{a}{g'} & \frac{d^2}{dZ^2} + \frac{\omega_-^0}{(g')^2} \end{pmatrix} \cdot \begin{pmatrix} a_{\mathbf{k}}^0 \\ b_{\mathbf{k}}^0 \end{pmatrix} = \begin{pmatrix} 0 \\ 0 \end{pmatrix}. \quad (\text{A7})$$

We now make the ansatz $a_{\mathbf{k}}^0(z, Z) = a_{\mathbf{k}}^{0,0}(z) \exp(iZ)$ and find that the scaling function g is chosen such that

$$((g')^2 - \omega_-) ((g')^2 - \omega_+) = p^4 + (ag')^2 \quad (\text{A8})$$

and $Z = \frac{1}{\epsilon} \int^z dx g'(x)$, so that the adiabatic solution is

$$A_{\mathbf{k}}(z) \sim a_0(z) \exp\left(\int^z dx g'(x)\right). \quad (\text{A9})$$

Similarly we can find a solution for $B_{\mathbf{k}}(z)$. Disregarding tunneling states which only give an exponentially small contribution to the conductance, the number of propagating modes is determined by the condition $\text{Im}[g'(x)] = 0$. From (A8), we see that the number of propagating modes is determined by the position where $a(z)$ attains its maximum, *i.e.* the conductance can be calculated as for a spin-spiral with $a(z) \rightarrow a_{\text{max}}$.

APPENDIX B: FREQUENCY SUMMATIONS

The typical frequency sum to be performed is

$$\pi^l = \frac{1}{\beta} \sum_n X^{n+l} Y^n + (l \rightarrow -l), \quad (\text{B1})$$

where X^n and Y^n are Matsubara Green's functions. They can be written in the spectral representation

$$X^n = \int_{-\infty}^{\infty} \frac{d\epsilon}{2\pi} \frac{S_X(\epsilon)}{i\omega_n - \epsilon}, \quad (\text{B2})$$

where the spectral function is determined by the retarded and the advanced function

$$S_X(\epsilon) = i [X^R(\epsilon) - X^A(\epsilon)]. \quad (\text{B3})$$

Performing the frequency summation in (B1), we get

$$\pi^l = \int_{-\infty}^{\infty} \frac{d\epsilon_1}{2\pi} \int_{-\infty}^{\infty} \frac{d\epsilon_2}{2\pi} S_X(\epsilon_1) S_Y(\epsilon_2) \times \left[\frac{f(\epsilon_2) - f(\epsilon_1)}{i\omega_l - (\epsilon_1 - \epsilon_2)} - \frac{f(\epsilon_1) - f(\epsilon_2)}{i\omega_l - (\epsilon_2 - \epsilon_1)} \right]. \quad (\text{B4})$$

The DC-conductivity is obtained by an analytical continuation

$$I \equiv - \lim_{\omega \rightarrow 0} \frac{\pi^l(i\omega_l \rightarrow \omega + i\delta)}{\omega} \quad (\text{B5})$$

and we consider the limit of zero temperature ($T \rightarrow 0$):

$$I = \frac{\hbar}{2\pi} S_X(0) S_Y(0) \quad (\text{B6})$$

$$= \frac{\hbar}{\pi} \text{Re} [X^R(0) Y^A(0) - X^R(0) Y^R(0)]. \quad (\text{B7})$$

The product of the two retarded (advanced) Green's functions vanishes when integrating over the energy since the poles are on the same side of the imaginary plane. The sum can then be simplified to

$$I = \frac{\hbar}{\pi} \text{Re} [X^R(0)Y^A(0)] . \quad (\text{B8})$$

This relation will be used in the following in order to calculate the contributions from the diagrams 1–5.

We use

$$G_{s'}^R(0)G_s^A(0) = \frac{G_{s'}^R(0) - G_s^A(0)}{-i(\delta_s + \delta_{s'}) - (\epsilon^s - \epsilon^{s'})} , \quad (\text{B9})$$

where $\delta_s = \hbar/(2\tau_s)$ and obtain in the limit $\delta_s \ll \mu$ the contribution from π_1 to the conductivity

$$I_1 \approx [1 + (\frac{\epsilon^s - \epsilon^{s'}}{\delta_s + \delta_{s'}})^2]^{-1} \frac{\tau_s \tau_{s'}}{\tau_s + \tau_{s'}} [\delta(\xi^{s'}) + \delta(\xi^s)] , \quad (\text{B10})$$

where $\xi^s = \epsilon^s - \mu$ is the quasiparticle energy relative to the Fermi level. In the case of no spin-splitting ($\xi^s \rightarrow \xi$) and ($\delta_s \rightarrow \delta$), the result is $I_1 \approx \tau \delta(\xi)$. In the limit of strong spin-splitting, the result is vanishing small (of order $\hbar/\Delta\tau$ small).

$$I_1 \approx 0 . \quad (\text{B11})$$

The sum π^2 gives a contribution

$$I_2 = \frac{\hbar}{2\pi} \frac{\partial}{\partial \xi^s} \frac{1}{(\xi^s)^2 + \delta_s^2} \approx \tau_s \frac{\partial}{\partial \xi^s} \delta(\xi^s) . \quad (\text{B12})$$

The sum π^3 gives a contribution

$$I_3 = -\frac{\hbar}{\pi} \frac{1}{(\xi^s)^2 + \delta_s^2} \frac{\xi^{-s}}{(\xi^{-s})^2 + \delta_{-s}^2} . \quad (\text{B13})$$

In the limit of vanishing spin-splitting and equal lifetimes, the contribution is $I_3 \approx \tau(\partial/\partial \xi)\delta(\xi)$, which agrees with the result of π_2 as it should. When $\Delta\tau_s/\hbar \gg 1$ (large spin-splitting) it is

$$I_3 \approx -\frac{2\tau_s}{\epsilon^{-s} - \epsilon^s} \delta(\xi^s) . \quad (\text{B14})$$

In the case of no spin-splitting, the sum π^4 gives a contribution

$$I_4 \approx \hbar \left[-\frac{1}{4} \delta(\xi) \delta^{-3} + \frac{1}{8} \delta''(\xi) \delta^{-1} \right] . \quad (\text{B15})$$

In the general case, we use

$$G_{s'}^R(0)G_{-s}^R(0) = \frac{G_s^R(0) - G_{-s}^R(0)}{i(\delta_{-s} - \delta_s) - (\epsilon^{-s} - \epsilon^s)} . \quad (\text{B16})$$

For large splitting the result is then

$$I_4 \approx \frac{-\tau_s}{\epsilon^{-s} - \epsilon^s} \delta'(\xi^s) - \frac{2\tau_s}{(\epsilon^{-s} - \epsilon^s)^2} \delta(\xi^s) + \frac{\tau_s \left(1 - \frac{\tau_s}{\tau_{-s}}\right)}{(\epsilon^{-s} - \epsilon^s)^2} \delta(\xi^s) . \quad (\text{B17})$$

Finally, the sum π_5 gives a contribution

$$I_5 = \frac{\hbar}{2\pi} \frac{1}{(\xi^s)^2 + \delta_s^2} \frac{1}{(\xi^{-s})^2 + \delta_{-s}^2} . \quad (\text{B18})$$

In the case of no spin-splitting the sum is

$$I_5 \approx \hbar \left[\frac{1}{4} \delta(\xi) \delta^{-3} + \frac{1}{8} \delta''(\xi) \delta^{-1} \right] . \quad (\text{B19})$$

For large spin-splitting, we have

$$I_5 \approx \frac{1}{(\epsilon^s - \epsilon^{-s})^2} [\tau_s \delta(\xi^s) + \tau_{-s} \delta(\xi^{-s})] . \quad (\text{B20})$$

APPENDIX C: SPIN SPIRAL

The spin-spiral system has a constant gradient of the rotating magnetization direction ($a_q = a_0 \delta_{q,0}$). We perform the local gauge transformation (2). The transformed Hamiltonian is

$$\tilde{H} = \frac{\hbar^2}{2m} \sum_{\mathbf{k}} \mathbf{c}_{\mathbf{k}}^\dagger \left(k^2 - \sigma_z p^2 + a_0 k_z \sigma_y + \frac{1}{4} a_0^2 \right) \mathbf{c}_{\mathbf{k}} , \quad (\text{C1})$$

where $\mathbf{c}_{\mathbf{k}}$ is an annihilation operator in the spinor spin-space and the exchange splitting $\Delta \equiv \hbar^2 p^2/(2m)$ has been introduced. The transformed current operator is

$$J = \frac{e\hbar}{m} \sum_{\mathbf{k}} \mathbf{c}_{\mathbf{k}}^\dagger \left(k_z + \frac{a_0}{2} \sigma_y \right) \mathbf{c}_{\mathbf{k}} . \quad (\text{C2})$$

The Hamiltonian (C1) can be exactly diagonalized, and the eigenvalues are

$$E_{\mathbf{k}}^\pm = \frac{\hbar^2}{2m} \left(k^2 + \frac{1}{4} a_0^2 \mp \sqrt{k_z^2 a_0^2 + p^4} \right) \quad (\text{C3})$$

with the corresponding eigenvectors

$$\mathbf{u}_\pm = \mathcal{N}_\pm \begin{pmatrix} 1 \\ i(1 \mp \sqrt{1 + \alpha^2})/\alpha \end{pmatrix} , \quad (\text{C4})$$

where the parameter $\alpha \equiv k_z a_0/p^2$ is introduced and the normalization factors are

$$\mathcal{N}_\pm^2 = \frac{\alpha^2}{2\sqrt{1 + \alpha^2}(\mp 1 + \sqrt{1 + \alpha^2})} . \quad (\text{C5})$$

The annihilation operators are transformed as $\mathbf{c} = (\mathbf{u}_+, \mathbf{u}_-) \mathbf{a}$. In the new basis, the current operator is

$$\tilde{J} = \frac{e\hbar}{m} \sum_{\mathbf{k}} \mathbf{a}_{\mathbf{k}}^\dagger \begin{pmatrix} k_z - \frac{a_0 \alpha}{2\sqrt{1 + \alpha^2}} & \frac{a_0}{2\sqrt{1 + \alpha^2}} \\ \frac{a_0}{2\sqrt{1 + \alpha^2}} & k_z + \frac{a_0 \alpha}{2\sqrt{1 + \alpha^2}} \end{pmatrix} \mathbf{a}_{\mathbf{k}} \quad (\text{C6})$$

The DC conductivity is

$$\sigma = \frac{1}{4\pi} \frac{\hbar}{V} \sum_{\mathbf{k}ss'} |J_{ss'}|^2 A_{\mathbf{k}}^s A_{\mathbf{k}}^{s'}, \quad (\text{C7})$$

where the electron spectral function ($A = -2\text{Im}G^R$) at the Fermi level is

$$A_{\mathbf{k}}^s = \frac{\hbar/\tau}{(E_{\mathbf{k}}^s - \mu)^2 + (\hbar/\tau)^2}. \quad (\text{C8})$$

Here we have inserted a phenomenological scattering lifetime, which is identical for the two eigenstates. Note that we cannot treat different scattering life-times for the minority and majority states in the bulk ferromagnet with the method outlined in this appendix, since the life-times appearing in (C7) are the life-times for the exact eigenstates in the spin-spiral. In order to determine the relation between the different lifetimes, the general method described above in our paper should be used. From (C7) and (C8) it can be seen that the off-diagonal terms in the conductivity, $A_+ A_-$ are in the order $1/(\tau\Delta/\hbar)^2$ smaller than the diagonal terms. We further assume that the scattering by the domain wall is weak, *i.e.* $a_0^2 \ll p^2$ and $a_0 k_F^s \ll p^2$ and expand the result for the conductivity to the second order in a_0 . The conductivity becomes

$$\sigma = \frac{e^2 \tau}{6\pi^2 m} \sum_s \left(k_\mu^2 - \frac{a_0^2}{4} + sp^2 \right)^{3/2} \left(1 - \frac{sE_w}{4\Delta} \right), \quad (\text{C9})$$

where $\hbar^2 k_\mu^2/(2m) = \mu$ and $E_w = \hbar^2 a_0^2/(2m)$ are used. The conductivity should be related to the electron density by eliminating any reference to the chemical potential which may change in the presence of the domain wall,

$$n_s = \frac{1}{6\pi^2} \left(k_\mu^2 - \frac{a_0^2}{4} + sp^2 \right)^{3/2} \left(1 + \frac{sE_w}{4\Delta} \right). \quad (\text{C10})$$

Inserting (C10) into (C9), the conductivity can therefore be written as

$$\sigma = \sigma_0 \left(1 - \frac{n_+ - n_-}{n_+ + n_-} \frac{E_w}{2\Delta} \right), \quad (\text{C11})$$

where $\sigma_0 = e^2(n_+ + n_-)\tau/m$ is the Drude conductivity. The domain wall resistivity, $\rho_w = -\delta\sigma_w/\sigma_0^2$ is thus

$$\rho_w = \frac{e^2 \rho_0^2 E_w}{2m\Delta} (n_+ - n_-), \quad (\text{C12})$$

where $\rho_0 = 1/\sigma_0$.

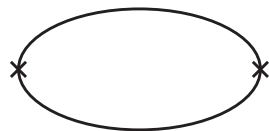
[†] also at Philips Research Laboratories, Prof. Holstlaan 4, 5656 AA Eindhoven, The Netherlands.

- ¹ J.F. Gregg, W. Allen, K. Ounadjela, M. Viret, M. Hehn, S. M. Thompson and J. M. D. Coey, Phys. Rev. Lett. **77**, 1580 (1996) ; M. Viret, D. Vignoles, D. Cole, J. M. D. Coey, W. Allen, D. S. Allen and J. F. Gregg, Phys. Rev. B **53**, 8464 (1996).
- ² K. M. Hong, N. Giordano, J. Phys.: Condensed Matter, **10**, L401 (1998).
- ³ Y. Otani, S. G. Kim, K. Fukamichi, O. Kitakami and Y. Shimada, IEEE Trans. Magn., **34**, 1096 (1998).
- ⁴ A. D. Kent, U. Ruediger, J. Yu, S. Zhang, P. M. Levy, Y. Zhong and S. S. P. Parkin, IEEE Trans. Magn., **34**, 900 (1998); U. Ruediger, J. Yu, S. Zhang, A. D. Kent, S. S. P. Parkin, Phys. Rev. Lett., **80**, 5639 (1998); A. D. Kent, U. Ruediger, J. Yu, L. Thomas and S. S. P. Parkin cond-mat/9812163.
- ⁵ R. P. van Gorkom, J. Caro, S. J. C. H. Theeuwens, K. P. Wellok, N. N. Gribov, Appl. Phys. Lett. **74**, 422 (1999).
- ⁶ G. Tatara and H. Fukuyama, Phys. Rev. Lett. **67**, 3773 (1997).
- ⁷ P.M. Levy and S. Zhang, Phys. Rev. Lett. **79**, 5110 (1997)
- ⁸ J. van Hoof, K. M. Schep, A. Brataas, G. E. W. Bauer and P. J. Kelly Phys. Rev. B **59**, 138 (1999).
- ⁹ N. Garcia, M. Muñoz, and Y.-W. Zhao, Phys. Rev. Lett. **82**, 2923 (1999).
- ¹⁰ G.G. Cabrera and L.M. Falicov, Phys. Stat. Sol. B **62**, 217 (1974); **61**, 539 (1974).
- ¹¹ L. Berger, J. Appl. Phys. **55**, 1954 (1984).
- ¹² U. Ruediger, J. Yu, S. S. P. Parkin and A. D. Kent, in press.
- ¹³ U. Ruediger, J. Yu, L. Thomas, S. S. P. Parkin and A. D. Kent cond-mat/9901245.
- ¹⁴ A. Brataas, G. Tatara and G. E. W. Bauer, Phil. Mag. B **78**, 545 (1998).
- ¹⁵ I. Mertig, R. Zeller and P. H. Dederichs, Phys. Rev. B **49**, 11767 (1994); P. Zahn, I. Mertig, M. Richter and H. Eshrig, Phys. Rev. Lett. **75**, 2996 (1995).
- ¹⁶ C. M. Bender and S. A. Orszag, *Advanced Mathematical Methods for Scientists and Engineers* (McGraw-Hill, New York, 1978).

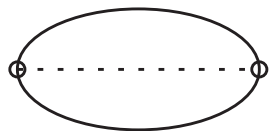
FIG. 1. Feynman diagrams of the contributions to the conductivity to the lowest order in the domain wall scattering. Solid lines indicate the electron Green's function and the dashed lines the interaction with the domain wall. The vertex \times arises from the unperturbed current operator (8), the vertex \circ is due to the gauge transformation on the current operator (9), the vertex \diamond is due to the first term in the interaction Hamiltonian (4) and the vertex \square is due to the second term in the interaction Hamiltonian (4).

FIG. 2. Feynman diagrams of the contributions to the electron density to the lowest order in the domain wall scattering. Solid lines indicate the electron Green's function and the dashed lines the interaction with the domain wall. The vertex \diamond is due to the first term in the interaction Hamiltonian (4) and the vertex \square is due to the second term in the interaction Hamiltonian (4).

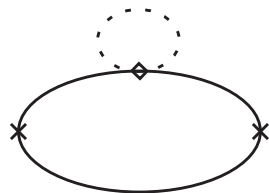
FIG. 3. The relative change in the resistivity, $\rho_w/(\kappa\rho_0)$, due to the scattering by the domain wall as a function of the asymmetry in the scattering life-times τ_+/τ_- . The solid line is for $\gamma = k_F^+/k_F^- = 1.01$, the dashed line is for $\gamma = k_F^+/k_F^- = 1.20$ and the dotted line is for $\gamma = k_F^+/k_F^- = 10.0$.



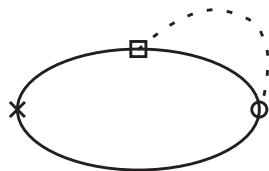
(0)



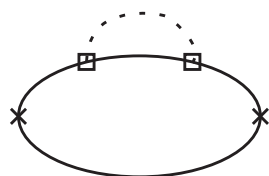
(1)



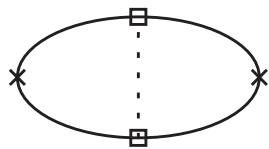
(2)



(3)



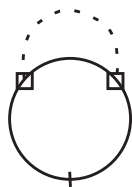
(4)



(5)



(A)



(B)

